

# New Testing in Support of LS-DYNA MAT 224 Material Model

Amos Gilat, Jeremy Seidt, Nathan Spulak, Jarrod Smith

The Ohio State University  
Department of Mechanical and Aerospace Engineering  
Columbus OH, USA

## 1 Abstract

LS-DYNA MAT224 is a tabulated plasticity and failure model. The plasticity part of the model can include strain rate, strain hardening and temperature effects, and the failure part is based on a failure surface of the equivalent plastic strain to failure as a function of triaxiality and the Lode parameter. The present paper presents two new experiments that have been developed recently in order to support the model. The first experiment adds new points to the failure surface in a region that is important in simulations of projectile impact and penetration. The second experiment is used for determining the Taylor-Quinney coefficient ( $\beta$ ), which controls the magnitude of the temperature increase due to plastic deformation.

Simulations of impact and penetration events show that failure occurs under a stress state of biaxial tension and out-of-plane compression. This state of stress on the failure surface is not in the region that is populated with data points obtained from typical experiments (tensile tests of flat and round, parallel and notched specimens, tensile tests of wide parallel and notched specimens, pure shear tests, combined tension-compression/shear tests, and compression tests.) In order to obtain an independent measurement of the equivalent strain to failure under a state of stress of biaxial in-plane tension and out-of-plane compression a new experiment was developed. In this experiment a small diameter punch penetrates a thin specimen plate that is backed by another plate. The deformation of the back surface of the plate is measured with DIC. The value of the equivalent strain to failure is determined from measuring the force and matching the LS-DYNA simulation with the measured deformation and force.

Plastic deformation generates heat and the fraction of the plastic work that is dissipated by heat is given by the Taylor-Quinney coefficient ( $\beta$ ). Temperature increase during plastic deformation softens the material and can offset the increase of stress due to strain hardening. Knowledge of the value of  $\beta$  is essential in numerical simulations of applications that involve dynamic loading since in these applications there is not sufficient time for the heat to dissipate and the temperature rise can be significant. A new test for determining the value of  $\beta$  is presented. In this test a material coupon specimen is loaded in tension at high strain rate. Full field measurements of deformation and temperature throughout the test (including in the necking region during the localization) are used for determining the value of  $\beta$  as a function of strain. Results from tests with specimens made of AISI 316L austenitic stainless steel show that the value of  $\beta$  increases with strain and reaches a plateau value of about 0.7 at strain of about 0.3. During the localization (necking) that follows, the value of  $\beta$  increases above 0.9.

## 2 New points on the MAT224 failure surface

The MAT\_224 material model (also known as MAT\_TABULATED\_JOHNSON\_COOK) in LS-DYNA is a tabulated plasticity and ductile failure model for metals. The plasticity part of the model, which is based on the Johnson Cook model [1], is strain rate, strain hardening, and temperature dependent, and requires input of stress strain curves from tests at various temperatures and strain rates. The ductile failure part of the model is based on a failure surface that gives the equivalent plastic failure strain as a function of triaxiality  $\sigma^*$  and Lode parameter  $\mu$ , which are defined by:

$$\sigma^* = \frac{p}{\sigma_{vm}}, \quad \mu = \frac{27}{2} \frac{J_3}{\sigma_{vm}^3} \quad (1)$$

Where  $p$  is the hydrostatic pressure (mean stress),  $\sigma_{vm} = \left( \frac{3}{2} s_{ij} s_{ij} \right)^{1/2}$  is the Von Mises equivalent stress ( $s_{ij} = \sigma_{ij} - \frac{1}{3} \sigma_{kk} \delta_{ij}$  are the components of the deviatoric stress tensor), and  $J_3 = \frac{1}{3} s_{ij} s_{jk} s_{ki}$  is the third

invariant of the deviatoric stress tensor. The data points that make up the failure surface are obtained from tests in which specimens are loaded and deform to failure under different combinations of stresses. The tests are simulated numerically such that the measured and calculated displacement and loads match. The calculated plastic strains at the failure point are then used as the value of the equivalent failure strain that is used in the failure surface. Tests that are typically used for creating the failure surface include tensile tests of round and flat notched specimens (with different notch geometries), combined tensile and compression tests, and shear tests, and tensile tests of flat wide notched specimens (with different notch geometries).

Simulations of ballistic impact experiments with plates made of 2024 aluminum [2] showed that fracture occurred at points where the Lode parameter equals -1 and the triaxiality values are near zero. The tests that are typically used in creating the failure surface do not produce data points in this region of triaxiality and Lode parameter. This region of the failure surface has been theoretically and numerically investigated recently [3] where it was shown that the state of stress corresponds to biaxial tension and out-of-plane compression. It was also suggested [3], that a small diameter punch test of a thin plate and of a thin plate backed by another plate can potentially be used for obtaining new data points in this region. The testing configuration is shown schematically in Figure 1.

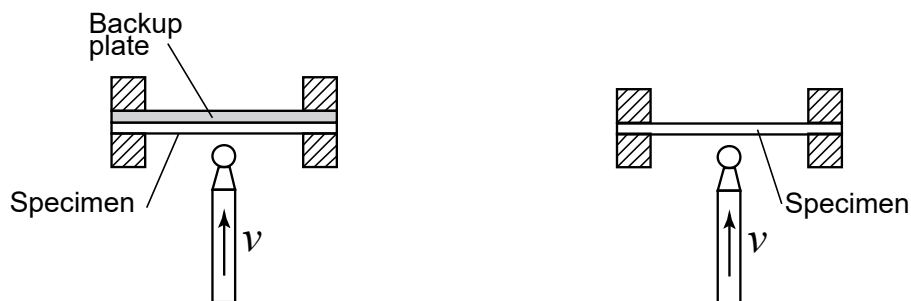


*Fig. 1: Schematics of the backed (left) and unbacked (right) small-diameter punch test.*

In the unbacked tests the Digital Image Correlation (DIC) technique was used to measure the deformation at the back surface of the plate. Two types of tests, interrupted and uninterrupted, were conducted with the backup plate configuration. In the uninterrupted tests the punch was loading the specimen continuously. The displacement of the punch and the force were recorded during the test and the values were compared with numerical simulations. In the interrupted tests the back side of the specimen plate was painted with a speckle pattern. Loading of the specimen was done sequentially in steps. After each step the specimen plate was taken out, a photo of the deforming speckle pattern was taken, and the specimen was examined to see if it was fractured. The history of the loading and deformation was compared with the simulations and the value of the calculated strains where fracture was observed was taken as the value for the new data point. Examples of measured and calculated data are shown in Figures 2 and 3. Figure 2 shows a comparison of the measured and calculated load versus strain history from an unbacked test, and Figure 3 shows the full-field DIC measured strain and the full-field calculated strain near the end of the test.

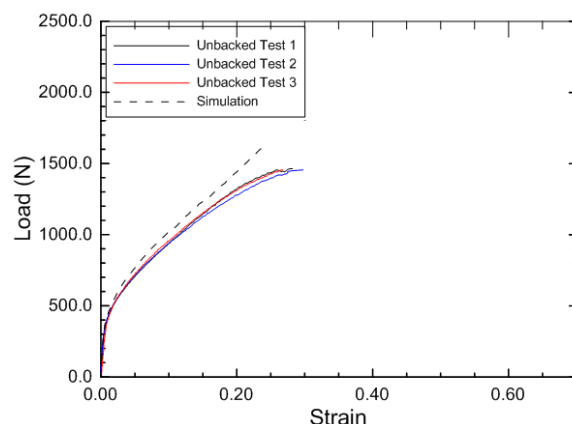


*Fig. 2: Measured and simulated load versus strain in a unbacked experiment.*

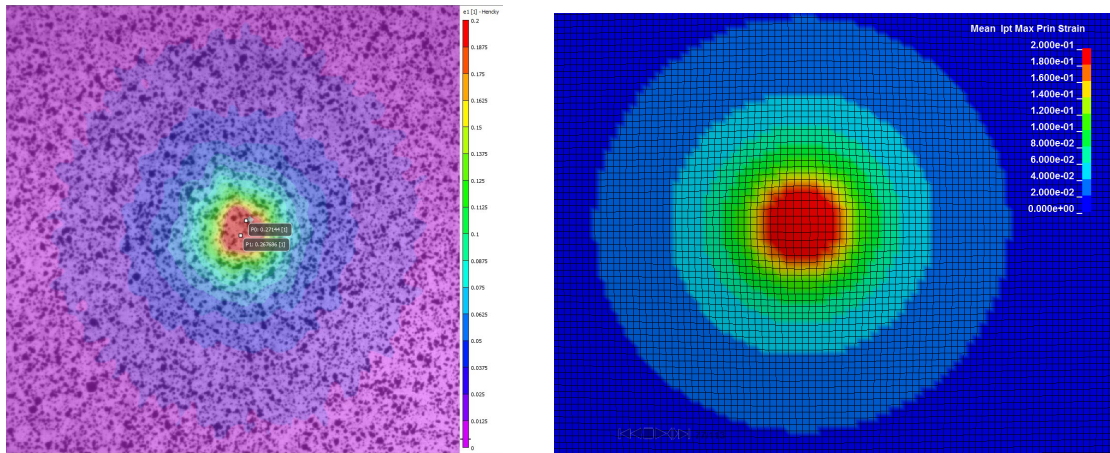


*Fig.3: Full-field strain during an unbacked experiment, DIC (left), simulation (right).*

### 3 Measuring the Taylor-Quinney Coefficient

As mechanical work is done on the material, a portion of the work is spent to deform the microstructure and increase the stored energy while a larger portion is dissipated as heat to the surroundings. The fraction of plastic work that is converted to heat during deformation is often denoted by the variable  $\beta$  and is known as the Inelastic Heat Function (IHF) or the Taylor Quinney coefficient [4, 5]. In these experiments  $\beta$  was determined to be a constant 0.8-0.9 for all metals, however, these first tests were performed quasi-statically at low levels of strain using complex calorimeter setups. The present paper presents a new experimental setup for determining the Taylor Quinney coefficient. In this setup the Taylor Quinney coefficient is determined from simultaneous measurements of full-field deformation and full-field temperature on the surface of a specimen during tensile tests. The setup consists of visual cameras on one side of the specimen and a high speed IR camera on the other side. Tests at quasi-static stain rate were done using a servo-hydraulic load frame. Tests at a dynamic strain rate were done using a special intermediate strain rate apparatus [6]. The specimen geometry is shown in Figure 4, and photographs of the static and dynamic experimental setups are shown in Figure 5.

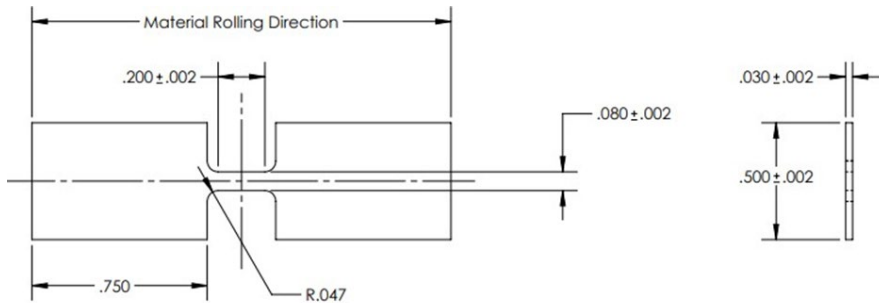


*Fig.4: Specimen geometry (dimensions in inches).*

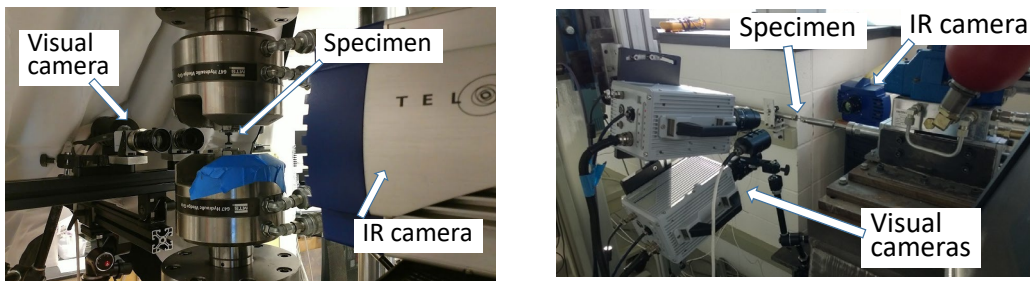


*Fig.5: Experimental setup, Quasi-static (left) dynamic (right).*

The quasi-static tests were done with the specimens deforming at a nominal strain rate of  $1 \text{ s}^{-1}$ . Vision Research Phantom v7.3 cameras were used for the DIC with pixel resolution of  $800 \times 600$  and speed of 500 fps. The temperature was measured with a Telops FAST-IR camera with pixel resolution of  $256 \times 320$  and speed of 500 fps. The dynamic tests were done with the specimens deforming at a nominal strain rate of  $200 \text{ s}^{-1}$ . Vision Research Phantom v7.3 cameras were used for the DIC with pixel resolution of  $450 \times 250$  and speed of 20,000 fps. The temperature was measured with a Telops FAST-IR camera with pixel resolution of  $64 \times 128$  and speed of 10,000 fps. Images of the deformation (DIC axial strain) and temperature recorded during the quasi-static and dynamic tests are shown in Figure 6

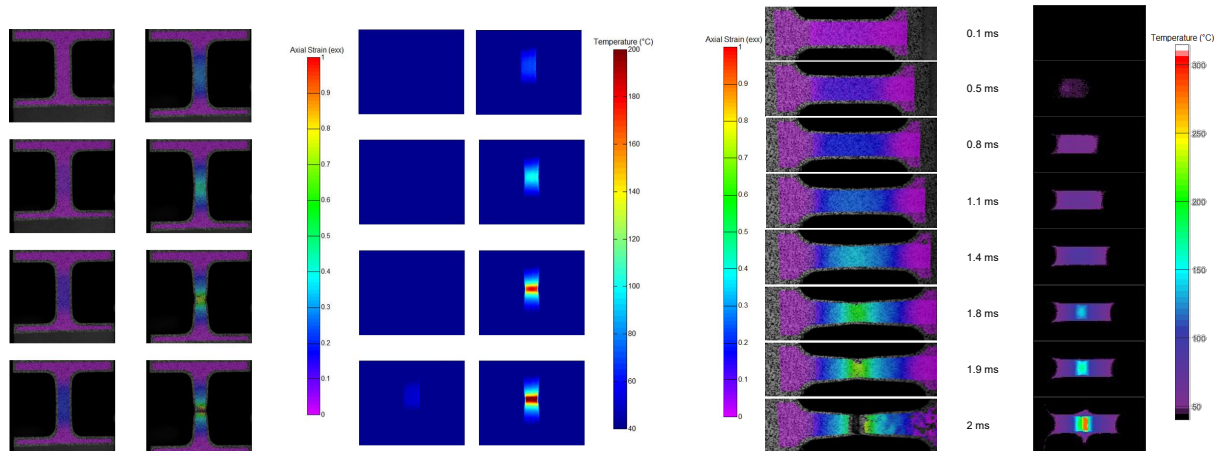


Fig.6: Axial strain (DIC) and temperature measurements, Quasi-static (left) dynamic (right).

Waterfall plots of the history of the axial strain and the temperature along the specimen's centerline are shown in Figure 7 and Figure 8 for the quasi-static and dynamic tests, respectively.

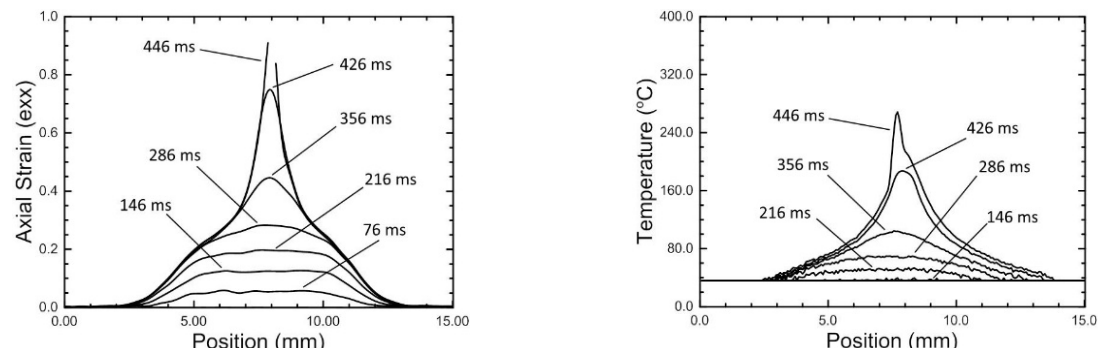


Fig.7: Axial strain and temperature history along the specimen's center line during quasi-static test.

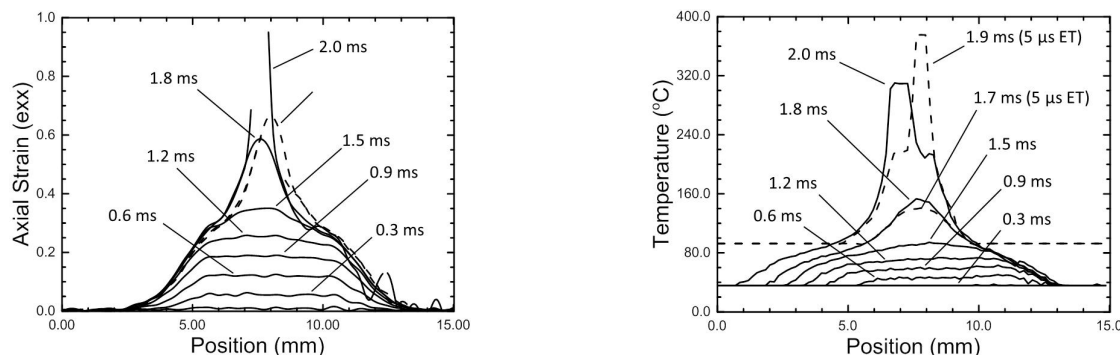


Fig.8: Axial strain and temperature history along the specimen's center line during dynamic test.

The figures show a nearly uniform deformation up to about a strain of 0.3 when necking starts to develop. At that stage the temperature has increased from room temperature to about 80°C. Once the necking starts the deformation localizes with strain exceeding 0.6 and temperature reaching about 250°C in the 1 s<sup>-1</sup> strain rate test and about 350°C in the 200 s<sup>-1</sup> strain rate test. An approximate calculation of the Taylor-Quinney coefficient ( $\beta$ ) is done by calculating the plastic work from estimating the average stress and strain in the middle of the neck. Figure 9 shows the calculated values from the 1 s<sup>-1</sup> and 200 s<sup>-1</sup> strain rate tests as a function of strain throughout the tests. (In the 1 s<sup>-1</sup> strain rate test a change of temperature is first detected when the strain is about 0.12.) The results show that, at both strain rates, during the uniform deformation  $\beta$  increases with strain and reaches a stable value of about 0.7 at a strain of 0.2. Once the necking starts at a strain of about 0.3 and the deformation localizes  $\beta$  increases. In the 200 s<sup>-1</sup> test  $\beta$  reaches a value of about 0.97. In the 1 s<sup>-1</sup> test the increase of  $\beta$  is more gradual and  $\beta$  reaches a value of about 0.89 at the end of the test. One reason for the difference is probably the time scale of the tests. The low strain rate test is much slower and some of the heat that is generated during the necking is conducted away.

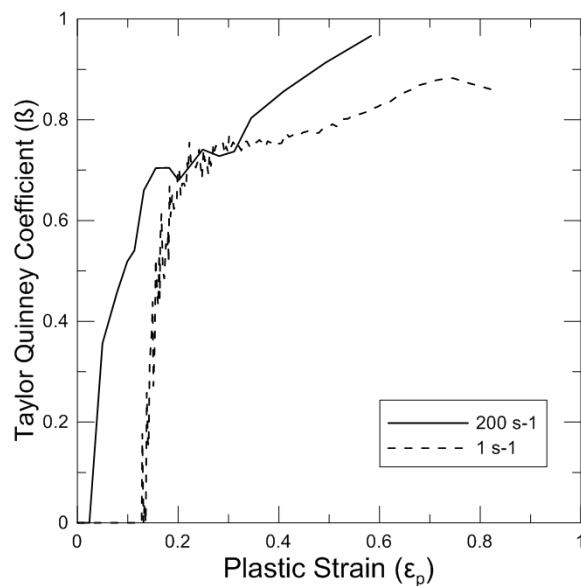


Fig.9: The Taylor Quinney coefficient for 316L austenitic stainless steel determined from quasi-static and dynamic tensile tests.

#### 4 Summary

To obtain accurate simulations, the tabulated LS-DYNA MAT224 plasticity and failure model requires significant amount of input data from tests with material coupon specimens. The plasticity part, which includes strain hardening, and strain rate and temperature effects, requires stress strain curves from tests at different stain rates and different temperatures. In the model (which is based on the analytical Johnson Cook model) the effects of hardening, strain rate and temperature are not coupled. In the tests that provide the data for the model these effects are coupled (e.g. the temperature during a high strain rate test increases during the test and therefore affecting the observed strain hardening). The accuracy of the simulations with MAT224 can be increased if thermal effects are included. Such simulations require knowledge of the Taylor Quinney coefficient and the present paper has presented a new experimental setup for measuring the coefficient.

The ductile failure part of the MAT224 model is based on a failure surface that give the equivalent plastic failure strain as a function of triaxiality and the Lode parameter. The surface is determined from data points that are obtained by loading to failure material specimens that are subjected to different combinations of stresses and matching the testing data to simulations. The present paper has presented a new testing configuration that provided data points to the failure surface in the region of Lode parameter equals -1 and the triaxiality values that are near zero. This state of stress corresponds to failure that occurs in plates subjected to ballistic impact.

## 5 Literature

- [1] Johnson, G.R., Cook, W.H., A constitutive model and data for metals subjected to large strains, high strain rates and high temperatures. In: Proceedings of the 7th International Symposium on Ballistics, The Hague, The Netherlands, 1983, 541-548
- [2] Pereira, J.M., Revilock, D.M., Ruggeri, C.R., Emmerling, W.C., and Altobelli, D.J., "Ballistic impact testing of aluminum 2024 and titanium 6AL-4V for material model development, ASCE J. of Aero. Eng., 27(3), 2014, 456-465
- [3] Lowe, R.L., Seidl, J.D., and Gilat, A., "Characterization of the Lode=-1 Meridian on the Al-2024 Failure Surface for \*MAT\_224 in LS-DYNA®. 14th International LS-DYNA Users Conference, 2016
- [4] Farren, W.S., Taylor G.I., "The heat developed during plastic extension of metals," Proc. R. Soc. A107, 1925, 422–451.
- [5] Taylor G.I., Quinney H, "The latent energy remaining in a metal after cold working," Proc. R. Soc. London 143, 1934, 307–326.
- [6] Gilat, A., Seidl, J.D. Matrika, Gardner, K.A, "A New Device for Tensile and Compressive Testing at Intermediate Strain Rates," Exp. Mech., to be published, 2019.